Article

Phase Stability Analysis: A Consistent Guide for Drawing Maps for Safe Traveling through the World of Azeotropy and Miscibility

Antonio Marcilla, Paloma Carbonell-Hermida, and María del Mar Olaya*
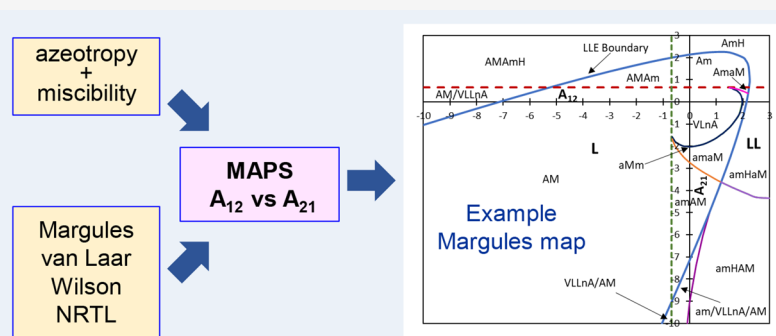
Read Online

ACCESS | Metrics & More | Article Recommendations | Supporting Information

ABSTRACT: Phase equilibria for systems that present different types of azeotropy have been analyzed by using the dimensionless Gibbs energy of mixing (g^M) for the liquid and vapor phases along with both the common tangent criterion and the phase stability test. First, the $g^{M,L}$ function for the liquid phase and its derivatives have been analyzed to obtain the boundary function between the homogeneous (L) and heterogeneous (LLE) regions as a function of the parameters for different activity coefficient models. Next, the excess Gibbs free energies and their first derivatives for the liquid and vapor phases have been analyzed to determine the mathematical conditions and the limits of different types of azeotropy (VLE and VLLE) and the possible combinations of two azeotropes in the same binary system. Finally, as a result of the combination of all this information, azeotropy and miscibility maps have been obtained as a function of the parameter values for Margules, van Laar, Wilson, and NRTL activity coefficient models.

1. INTRODUCTION

Correlation of phase equilibrium data plays an important role in the design and optimization of many separation processes, such as solvent extraction and rectification. Activity coefficient models are frequently used to describe the nonideal behavior of liquid mixtures. Margules,[1] van Laar,[2] Wilson,[3] and NRTL[4] are among the most popular of these models that have been used for a long time for liquid−liquid (LLE) and vapor−liquid (VLE) equilibrium data correlation (with the exception of the Wilson equation that cannot be used in LLE). These models with their corresponding parameters are implemented in the most popular simulation packages, such as Aspen Plus[5] and CHEMCAD,[6] to carry out phase equilibrium data calculations as those required for the simulation of chemical processes in which they are involved.

Although the theoretical background related to these topics seems to be well established, some important problems still remain unresolved. One of these problems is the lack of robustness in the algorithms frequently used for phase equilibrium data correlation, which results in convergence failures. During the optimization process involved in the correlation, a variety of phase behaviors are frequently analyzed and compared with the experimental one. For example, in VLE

(or VLLE), the systems may be zeotropic (nonazeotropic) or azeotropic; in the latter case, the azeotrope may be homogeneous of the global maximum or minimum boiling point, homogeneous of the intermediate boiling point, or otherwise heterogeneous. The complex optimization process involved in some cases may present convergence problems and could be interrupted at some point, especially for parameter values that are significantly different from those corresponding with the solution, where the equilibrium behavior can be very different from the experimental one. The probability of finding a solution to the correlation problem could be increased by using, during the optimization, an adequate strategy to *guide* and *restrict* the parameter values to those compatible with the specific phase equilibrium behavior to be correlated. In this way, a very interesting article has been published recently[7] connecting the parameter values of one of these models
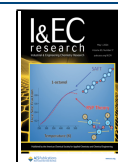
(NRTL) with the existence of the different homogeneous azeotropic behaviors that are possible in binary systems. This phenomenological study presented very valuable maps of the NRTL τ_{ij} parameter values (τ_{21} vs τ_{12}) producing different types of azeotropy. Also, the influence of the NRTL α_{ij} parameter and the importance of the vapor pressure of the pure components were discussed in this paper. Sapkowski and Hofman[8] applied a modified Equal Area Rule (EAR) algorithm to overcome some difficulties during the LLE calculations in binary systems and determined the range of NRTL parameters that reproduces different kinds of immiscibility. De Klerk and Schwarz[9] proposed a parametrization of the NRTL model (T$\tau\tau$) and applied it to the LLE of binary systems with upper and/or lower upper critical solution temperatures. This method decreases the complexity and computational requirements, reducing the nonlinear regression to two linear regression problems.

The phenomenon of azeotropy has been widely studied in the literature. Prediction of azeotropes without the requirement of VLE calculations is of interest to researchers. In some of these works, the objective is to obtain that data using a minimum of properties of the components of the system. For example, Brito Alves et al.[10] presented a neural network approach for the prediction of azeotrope formation using a series of macroscopic and microscopic properties of the pure components. Li et al.[11] proposed a method to predict homogeneous azeotropes in binary mixtures using pure component properties and activity coefficients at quasi-infinite dilution, which were estimated by the modified separation of cohesive energy density model, although any suitable method could be used. In other works, azeotropy is analyzed from a theoretical basis with the aim of calculating the conditions for such a phenomenon. Brandani[12] established the conditions for azeotrope formation at constant temperature in terms of the infinite dilution activity coefficients. In textbooks of thermodynamics, such as that of Gmehling and Kleiber,[13] the conditions for azeotropic behavior are also presented and discussed. Wisniak et al.[14] made a very comprehensive thermodynamical analysis of polyazeotropy at low pressures and established the conditions that cause it. The evolution of polyazeotropes with temperature and pressure was also discussed in that paper. Jaubert and Privat[15] published a note to clarify the relation between the sign (positive or negative) of the homogeneous azeotrope and the molar excess Gibbs energy (g^E) function. Bonilla-Petriciolet et al.[16] proposed a strategy based on the simulated annealing optimization technique to find homogeneous azeotropes in reactive and nonreactive mixtures. Skiborowski et al.[17] presented a unifying approach for the calculation of azeotropes for homogeneous and heterogeneous nonreactive mixtures based on an analogy of univolatility curves and the pinch branches for pure component products. Many other papers can be cited with different contributions to this matter.

In the present article, we use some of this previous information, combining and extending it with a new perspective, to establish the mathematical conditions that the typical activity coefficient models have to fulfill for the different types of azeotropy and miscibility behaviors. The aim of this work is to allow a better knowledge of the capabilities and limitations of such models to correlate phase equilibria (VLE, LLE, and VLLE) including the possible presence of more than one azeotrope and liquid splitting. For example, in the same way that dealing with LLE calculations is convenient to know

that the Wilson equation is not able to predict liquid–liquid (LLE) splitting, it would be very interesting to know, in advance of any equilibrium calculation, the region in the space defined by the model parameter values, where other models could lead to two or more LLE splitting with the possible presence of metastable solutions. Another example is in VLLE data fitting (e.g., with application in heterogeneous azeotropic distillation), where it would be very convenient to know the region where the parameters provide the heterogeneous azeotropic behavior for the model used as well as the type of binary azeotropy that the model may predict. The restriction of the model parameters during the correlation process to those values that correspond with the phase equilibrium behavior of the system would not only facilitate the search for the solution, but would also guarantee its consistency.[18,19]

In the present paper, a study was carried out to establish the relations between the parameter values of some of the most popular activity coefficient models and both the miscibility and azeotropic behavior of the mixtures. The models selected in this paper are Margules, van Laar, Wilson, and NRTL. The UNIQUAC model has not been included because the r_i and q_i structural parameters, required for each component of the system, restrict the possibility of generalization. However, the principles to deal with this model would be like those presented in this work. In the first part of this paper, the focus has been on the LLE to determine those functions between conjugate parameters that define, for each model, the boundary between one homogeneous liquid phase (L) region and two liquid phases in equilibrium (LLE) region. Next, the presence of a vapor phase (ideal) in equilibrium with one or more liquid phases has been considered. From this, maps showing those regions where the parameters provide different azeotropic and miscibility behaviors have been obtained for all the activity coefficient models selected. The Gibbs common tangent equilibrium condition, the stability test, as well as the comparison of the slopes of the Gibbs energy of mixing function (g^M) for the liquid and vapor phases, have been the tools used in the present work.

2. RESULTS

2.1. Liquid–Liquid Equilibrium. Phase equilibria can be analyzed very conveniently by using the dimensionless Gibbs energy of the mixing function ($g^M = G^M/RT$) along with the common tangent criterion and the stability test. Regarding liquid phases, a binary mixture is homogeneous (L) when the $g^{M,L}$ curve represented against composition (mole fraction, x_i) is convex over the whole composition domain. Figure S1a shows qualitatively the shape of this function and those of its first, second, and third derivatives with respect to composition (mole fraction, x_1). The first derivative ($dg^{M,L}/dx_1$) passes from negative to positive values and presents an "s" shape. The second derivative ($d^2g^{M,L}/dx_1{}^2$) is always positive and presents a minimum and, consequently, the third derivative ($d^3g^{M,L}/dx_1{}^3$) presents a shape similar to that of the first derivative with a zero at the mole fraction where the second derivative has the minimum. Figure S1b shows the corresponding representations for a system exhibiting liquid–liquid phase splitting (LLE). The $g^{M,L}$ curve shows convex/concave transitions. Consequently, the first derivative presents the "s" shape, but passes through a local maximum and a local minimum. Thus, the second derivative ($d^2g^{M,L}/dx_1{}^2$) presents two zeros, being negative in a certain interval of mole fractions. Figure S1c shows the conditions limiting the situations described in Figure

S1a,b, i.e., the limit between a system with no liquid phase splitting and with LLE. In this case, the first derivative presents an almost linear zone (limit where the local maximum and minimum vanish), and the second derivative minimum is zero, occurring at the same mole fraction where the third derivative is also zero, as Figure S1c shows. In the present article, these mathematical conditions have been used to calculate the boundary between the homogeneous (L) and heterogeneous (LL) regions of parameters for each selected activity coefficient model.

2.1.1. Margules Equation. In the following, the $g^{M,L}$ function according to the Margules equation is written as well as its second and third derivatives with respect to the composition for a binary system:

$$g^{M,L} = x_1 \ln x_1 + x_2 \ln x_2 + x_1 x_2 (A_{21} x_1 + A_{12} x_2) \tag{1}$$

$$\frac{d^2 g^{M,L}}{dx_1^2} = \frac{1}{x_1} + \frac{1}{x_2} - 2(A_{21} x_1 + A_{12} x_2) + 2(1 - 2x_1)$$
$$(A_{21} - A_{12}) \tag{2}$$

$$\frac{d^3 g^{M,L}}{dx_1^3} = -\frac{1}{x_1^2} + \frac{1}{x_2^2} - 6A_{21} + 6A_{12} \tag{3}$$

These equations are functions of the two binary interaction parameters (A_{12} and A_{21}) of the model and the mole fraction x_1 (with $x_2 = 1 - x_1$). The conditions to obtain the boundary function between the homogeneous (L) and heterogeneous (LL) regions are the equality of the second and third derivatives to zero at the same mole fraction (x_1^B), as shown in Figure S1c:

$$\left. \frac{d^2 g^{M,L}}{dx_1^2} \right|_{x_1^B} = 0 \tag{4}$$

$$\left. \frac{d^3 g^{M,L}}{dx_1^3} \right|_{x_1^B} = 0 \tag{5}$$

There are three unknowns (A_{12}, A_{21}, and x_1^B) but only two equations. So, the values for one of the parameters, A_{12} or A_{21}, have been set, and the other two, the binary interaction parameter and x_1^B, have been calculated by solving eqs 4 and 5 simultaneously. Table S1 and Figure 1 show the parameter values obtained for this boundary between the L and LL regions according to the Margules equation. For this equation, symmetry is observed about the bisectors to the first and third quadrants (dashed line in the figure). Taking into account this symmetry, the boundary obtained above the bisector has been fitted to the following sixth-degree polynomial equation (P_1):

$$A_{21} = P_1(A_{12})$$
$$= -1.335205 \times 10^{-5} A_{12}^6 - 3.871697 \times 10^{-4} A_{12}^5$$
$$- 4.186163 \times 10^{-3} A_{12}^4$$
$$-2.123819 \times 10^{-2} A_{12}^3 - 6.103912 \times 10^{-2} A_{12}^2$$
$$+ 1.836793 \times 10^{-1} A_{12} + 2.145975 \tag{6}$$

and below the bisector, the boundary accomplishes the polynomial P_2, which, considering the symmetry mentioned, has the same function as P_1:
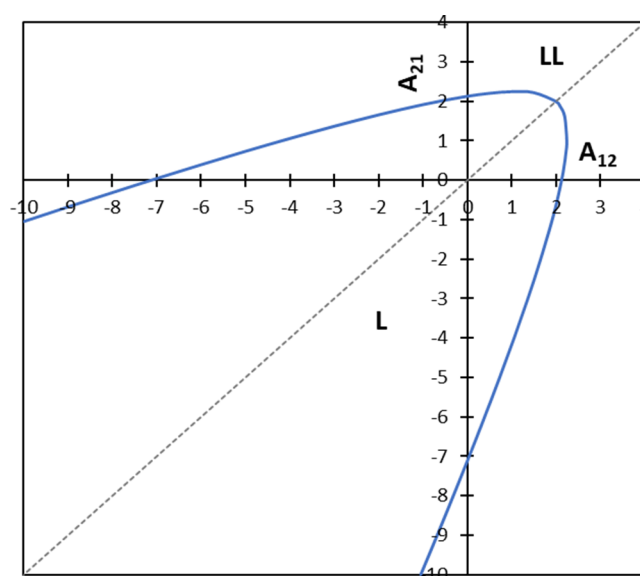
$$A_{12} = P_2(A_{21}) \tag{7}$$

Figure 1. Boundary (solid blue line) between the homogeneous (L) and heterogeneous (LL) regions for the Margules equation as a function of the binary interaction parameters A_{12} and A_{21}.

For A_{21} values higher than those obtained using the polynomial function of A_{12} shown in eq 6 ($A_{21} > P_1(A_{12})$), the liquid mixture will be unstable providing two liquid phases at equilibrium (LL region). For A_{21} values smaller than those calculated with eq 6 ($A_{21} < P_1(A_{12})$), a new value of the parameter A'_{12} has to be determined with the polynomial P_2 (eq 7) using the value of A_{21}. If $A'_{12} < P_2(A_{21})$, the system will be a homogeneous liquid phase (L), and if $A'_{12} > P_2(A_{21})$, the system splits into two liquid phases (LL).

Next, a similar procedure has been followed for the other activity coefficient models selected in this paper.

2.1.2. van Laar Equation. The van Laar equation for $g^{M,L}$ and its second and third derivatives with respect to composition (mole fraction) are presented in eqs S1−S4.

It should be considered at this point that the van Laar equation does not admit A_{12} and A_{21} parameters having different signs. In other words, only those combinations with both parameters being either positive (first quadrant) or negative (third quadrant) are possible. Besides, it has been checked in this work that the simultaneous solution to eqs 4 and 5 along with eqs S3 and S4 is only possible for both A_{12} and A_{21} values being positives. This means that the existence of liquid−liquid (LL) splitting is limited to some regions in the first quadrant of A_{21} versus A_{12}, while in the third quadrant, the solution is always a homogeneous liquid phase (L). Table S2 shows the values obtained for the boundary between the L and LL regions in the first quadrant, setting values for one of the two binary interaction parameters (A_{12} in this case) and calculating the other one (A_{21}) and x_1^B by solving eqs 4 and 5 along with eqs S3 and S4. This boundary between the L and LL regions, represented in Figure S2, has been fitted to the following third-degree polynomial equation:

$$A_{21} = P_3(A_{12})$$
$$= -4.828697 \times 10^{-2} A_{12}^3 + 3.395757 \times 10^{-2} A_{12}^2$$
$$- 5.666309 \times 10^{-1} A_{12} + 3.385391 \tag{8}$$

2.1.3. Wilson Equation. It is well-known that the Wilson equation does not provide LLE because the second derivative of the Gibbs energy of mixing is always positive (eqs S6 and S7). Consequently, any combination of parameters always provides a homogeneous liquid mixture (L region) for this model.

2.1.4. NRTL Model. The NRTL equation for a binary system and the second and third derivatives with respect to composition (x_1) are presented in eqs S8−S13.

For a binary system, this model has three parameters: τ_{12}, τ_{21}, and $\alpha_{12} = \alpha_{21}$. The boundary between the homogeneous (L) and heterogeneous (LL) liquid regions has been previously published[20] as a function of the nonrandomness parameter $\alpha_{12} = \alpha_{21}$. In the present paper, this boundary function has been calculated more precisely by solving eqs 4 and 5 along with eqs S12 and S13, for the specific value of $\alpha_{12} = \alpha_{21} = 0.2$, frequently used in the literature for LLE. Table S3 shows the parameter values, and the boundary curve has been represented in Figure S3. This curve has been fitted to a third-order polynomial equation, which is quite similar to the one previously published:

$$
\begin{aligned}
\tau_{21} &= P_4(\tau_{12}) \\
&= -2.150856\cdot10^{-3}\tau_{12}^3 + 6.904109\cdot10^{-2}\tau_{12}^2 \\
&\quad - 1.190333\tau_{12} + 2.609190
\end{aligned}
\tag{9}
$$

It is known that the NRTL model could produce, depending on the α_{ij} values, two different liquid−liquid (LL) splitting regions for a binary system, which could be both stable or, on the contrary, one of them metastable. Nevertheless, these regions have not been considered in the present analysis because they appear at very high and infrequent parameter values.[20]

2.2. Vapor−Liquid Equilibrium. Next, the vapor phase is considered and added to this study to obtain, for each one of the activity coefficient models selected, a map of the parameter values regarding the different possible combinations of liquid and vapor phases in equilibrium, with and without azeotropes of maximum or minimum temperature, which could also be either homogeneous or heterogeneous.

The Gibbs common tangent equilibrium condition along with the stability test can be applied to the liquid and vapor phases to establish the conditions for equilibrium (LLE, VLE, and VLLE). For this analysis, the Gibbs energies of both vapor and liquid phases must refer to the same reference state. The liquid phase at the same temperature and pressure of the mixture was selected as the reference state for each component. According to this selection, the Gibbs energy of mixing for the liquid phase $(g^{M,L})$ is given by eq 10, as a function of the mole fraction of the two components (z_i) and their activity coefficients (γ_i):

$$
g^{M,L} = g^{\text{ideal},L} + g^{E,L} = \sum_{i=1}^{2} z_i \ln z_i + \sum_{i=1}^{2} z_i \ln \gamma_i
\tag{10}
$$

That for the vapor phase $(g^{M,V})$, using the liquid phase as the reference and considering ideal vapor, is given by

$$
\begin{aligned}
g^{M,V} &\approx g^{M,\text{Videal}} \\
&= \sum_{i=1}^{2} z_i \ln z_i + \sum_{i=1}^{2} z_i g_i^{\text{pure},V} \\
&= \sum_{i=1}^{2} z_i \ln z_i + \sum_{i=1}^{2} z_i \ln \frac{P}{p_i^0}
\end{aligned}
\tag{11}
$$

where z_i is the mole fraction in any global mixture, γ_i is the activity coefficient, p_i^0 is the vapor pressure of component i, and P is the total pressure.

The representation of the Gibbs energy of mixing of the liquid phase $(g^{M,L})$ versus composition (z_1) is a curve passing through the $(0,0)$ and $(1,0)$ points. The representation of the Gibbs energy of mixing of the vapor phase $(g^{M,V})$ is the linear combination of an ideal term, similar to that of the liquid phase, and a straight line passing through the points $\left(0, \ \ln\left(\frac{P}{p_2^0}\right)\right)$ and $\left(1, \ \ln\left(\frac{P}{p_1^0}\right)\right)$. Figure S4 shows a possible representation of these two functions at a constant P for a zeotropic system. In Figure S4a, a constant temperature (T) is set with $T < T_{b,l}$ (boiling temperature of the light component), and so the liquid is the stable phase for any composition. Figure S4b shows the influence of the temperature in the $g^{M,V}$ function. Obviously, the curve moves downward in an almost parallel way as temperature increases. In this figure, the variation of the Gibbs energy of mixing of the liquid $(g^{M,L})$ with temperature has been neglected, which is a common practice in some equations (e.g., Margules or van Laar) or its influence is very weak in others (e.g., NRTL), and furthermore, it has no influence in the analysis that follows. In Figure S4c, both functions $(g^{M,L}$ and $g^{M,V})$ are represented at three temperatures, i.e., at the boiling points of the pure components (light $T_{b,l}$ and heavy $T_{b,h}$) and at an intermediate temperature (T_0) where a common tangent line to the two $g^{M,L}$ and $g^{M,V}$ curves can be drawn representing the minimum energy. The compositions of these two points with a common tangent line are the liquid and vapor phases at equilibrium (x_0, y_0) at T and P. At temperatures above $T_{b,h}$, the system is in the vapor phase, and at temperatures below $T_{b,l}$ is in the liquid phase, regardless of the composition.

The hypothetical system represented in Figure S4c would not have an azeotrope because it is not possible, at any temperature, to have a common tangent line to both the $g^{M,L}$ and $g^{M,V}$ curves at the same composition (z_1). Both curves can be tangent to each other only at $z_1 = 0$ (at $T = T_{b,h}$) or $z_1 = 1$ (at $T = T_{b,l}$). In this case, only one common tangent line exists between the $g^{M,V}$ and $g^{M,L}$ curves, at different compositions (x_0, y_0), at each temperature between the boiling points of both pure components.

Figure S5a shows an example of a binary system presenting VLE with one homogeneous azeotrope of minimum boiling point (Am). This situation is characterized by a temperature (T_{Am}), lower than $T_{b,l}$, where the $g^{M,V}$ and $g^{M,L}$ curves are tangent at an intermediate z_1 mole fraction. Figure S5b shows the corresponding situation for a binary system exhibiting one maximum boiling point azeotrope (AM) at a temperature (T_{AM}), higher than $T_{b,h}$, whereas Figure S5c shows the situation for a system with a heterogeneous azeotrope (AmH), which is always of minimum boiling temperature (T_{AmH}).

Other situations may occur, leading to systems with no azeotrope but with liquid−liquid−vapor equilibrium (VLLE)

or systems with two homogeneous azeotropes of global or local maximum or minimum temperatures, the last ones also called intermediate azeotropes. Figure S6 shows several possible cases. Figure S6a corresponds to a system with two azeotropes, one (global) maximum boiling point azeotrope (AM) at a low z_1 mole fraction and one (global) minimum boiling point azeotrope (Am) at a higher z_1 mole fraction. Figure S6b corresponds to one azeotrope of the (local) minimum boiling temperature (am) at low z_1 mole fraction and one (global) maximum boiling point azeotrope (AM) at high z_1 mole fraction. Finally, Figure S6c corresponds to one VLLE with no azeotrope (VLLnA) at compositions of x_0^I, x_0^{II}, and y_0 for the mole fractions of component 1 in the two liquids and one vapor phase in equilibrium, respectively. The temperature for this situation has been named T_{VLLnA} in Figure S6c.

Other behaviors may be possible, such as the combination of heterogeneous and homogeneous azeotropes. Nevertheless, because the analysis using the *excess* Gibbs free energy (for the liquid and vapor phases) is clearer for this aim than using the corresponding *mixing* functions, all possible cases of two azeotropes, including one homogeneous and one heterogeneous, will be presented from this point of view.

The occurrence of azeotropes of *global* minimum or maximum boiling temperatures is determined by the difference between the slopes of the tangent lines to the $g^{M,L}$ and $g^{M,V}$ curves at the extremes of the composition domain, i,e., at $z_1 = 0$ and $z_1 = 1$, being, for example, 1 the light component. To apply such analysis to specific systems, eqs 10 and 11 for $g^{M,L}$ and $g^{M,V}$, respectively, must be considered. The derivatives to be compared are

$$\left(\frac{dg^{M,L}}{dz_1}\right)_{z_1=1} \text{ and } \left(\frac{dg^{M,V}}{dz_1}\right)_{z_1=1} \tag{12}$$

$$\left(\frac{dg^{M,L}}{dz_1}\right)_{z_1=0} \text{ and } \left(\frac{dg^{M,V}}{dz_1}\right)_{z_1=0} \tag{13}$$

eqs 10 and 11 have a common term, the one that corresponds with the ideal contribution in the liquid phase that is given by eq 14, whose derivatives in both extremes ($z_1 = 1$ and $z_1 = 0$) represented by eq 15 are infinite:

$$g^{ideal} = \sum_{i=1}^{2} z_i \ln z_i \tag{14}$$

$$\left|\frac{dg^{ideal}}{dz_1}\right|_{z_1=1} = \left|\frac{dg^{ideal}}{dz_1}\right|_{z_1=0} = \infty \tag{15}$$

This fact leads to indeterminacy in the calculation of the derivatives given by eqs 12 and 13. Since the contribution represented by eq 14 is present in both $g^{M,L}$ and $g^{M,V}$ functions, eqs 10 and 11, respectively, and only the differences between their derivatives (not their own values) are of interest for the present analysis, the ideal term represented in eq 14 can be removed from both equations. Thus, the analysis can be done by comparing the excess Gibbs free energy of the liquid phase ($g^{E,L}$), represented by eq 16, and what could be considered as "pseudo excess" Gibbs free energy of the vapor phase ($g^{E,V}$), represented by eq 17, which is the result of considering the liquid phase as the reference state. In its strict sense, the excess contribution for the vapor phase is zero since ideal vapor has

been considered. However, by analogy with the liquid phase, the term represented in eq 17 has been labeled in this work as (pseudo) excess, E, for representing the difference among the total Gibbs free energy of the corresponding phase (liquid or vapor) and that represented by eq 14. Thus, the following equations and their corresponding derivatives are used in the analysis of azeotropy:

$$g^{E,L} = \sum_{i=1}^{2} z_i \ln \gamma_i \tag{16}$$

$$g^{E,V} = \sum_{i=1}^{2} z_i \ln \frac{P}{p_i^0} \tag{17}$$

The nomenclature used for the functions to compare is At $z_1 = 1$ and $T = T_{b,1}$

$$d_{L,1} = \left(\frac{dg^{E,L}}{dz_1}\right)_{z_1=1, T=T_{b,1}} \text{ and } d_{V,1} = \left(\frac{dg^{E,V}}{dz_1}\right)_{z_1=1, T=T_{b,1}} \tag{18}$$

At $z_1 = 0$ and $T = T_{b,2}$

$$d_{L,2} = \left(\frac{dg^{E,L}}{dz_1}\right)_{z_1=0, T=T_{b,2}} \text{ and } d_{V,2} = \left(\frac{dg^{E,V}}{dz_1}\right)_{z_1=0, T=T_{b,2}} \tag{19}$$

where $T_{b,1}$ and $T_{b,2}$ indicate the boiling temperatures for components 1 (light) and 2 (heavy), respectively, at the pressure of the system.

Figure 2 shows the $g^{M,L}$ and $g^{M,V}$ curves (Figure 2a1−c1), the $g^{E,L}$ curve and $g^{E,V}$ line (Figure 2a2−c2), their derivatives with respect to the mole fraction of the light component (z_1) (Figure 2a3−c3), and the temperature versus composition (z_1) diagram (Figure 2a4−c4), for a zeotropic binary system (case a), as well as for a system with one minimum boiling point
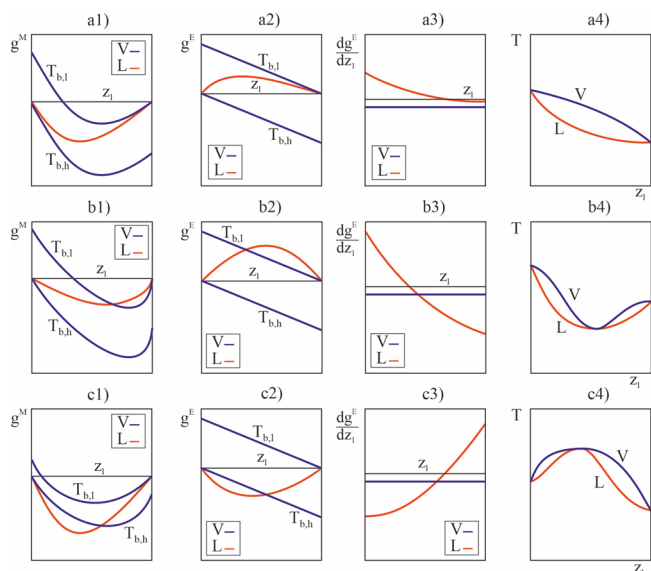

Figure 2. Representation of $g^{M,L}$ and $g^{M,V}$ curves (1), $g^{E,L}$ and $g^{E,V}$ functions (2), their derivatives with respect to the mole fraction of the light component z_1 (3), and T/z_1 diagram (4) for a binary system with (a) no azeotrope, (b) one Am, and (c) one AM.

azeotrope Am (case b), and another with one maximum boiling point azeotrope AM (case c).

If the system has no azeotropes, the derivative of $g^{E,L}$ does not intersect with that of $g^{E,V}$ (Figure 2a3), which is a constant value. To analyze the case represented in Figure 2b, the derivatives of $g^{M,L}$ and $g^{M,V}$ at $z_1 = 0$ and $z_1 = 1$ for a binary system that presents one minimum boiling point azeotrope (Am) are represented in Figure S7. In this figure, the Gibbs free energy of the mixing curve for the vapor, $g^{M,V}$, has been represented at two temperatures: the boiling temperatures of the light ($T_{b,l}$) and heavy ($T_{b,h}$) components. The slope of the g^M curve for both liquid and vapor phases is negative at $z_1 = 0$ and positive at $z_1 = 1$ and also tends to be infinite. Nevertheless, that of the vapor phase at both ends ($z_1 = 0$ for $T_{b,h}$ and $z_1 = 1$ for $T_{b,l}$) must be higher (in absolute value) than that of the liquid phase to guarantee the existence of one Am. In other words, the convexity of the vapor curve must be higher than that of the liquid phase, which, in turn, results in an intersection of the $g^{M,V}$ curve, calculated at the boiling point of the light component, to that of the liquid $g^{M,L}$ at a mole fraction between 0 and 1. To attain this situation, the $g^{E,L}$ curve must be positive and there must be one intersection point between the $g^{E,L}$ curve and the $g^{E,V}$ line in the positive domain (Figure 2b2). Thus, the first derivative of $g^{E,L}$ is a decreasing function intersecting that of $g^{E,V}$, which is constant (Figure 2b3). Following this reasoning, if the system presents one AM (Figure 2c), the $g^{E,L}$ curve must be negative, since the convexity of the $g^{M,L}$ curve must be higher than that of the $g^{M,V}$ curve. This is reflected in the existence of an intersection between the $g^{E,L}$ curve and the $g^{E,V}$ line in the negative domain (Figure 2c2). Thus, the first derivative of $g^{E,L}$ is an increasing function intersecting that of $g^{E,V}$ (Figure 2c3).

Accordingly, the required conditions for some of the most common VLE behaviors (totally miscible liquid phase) in terms of the derivatives presented in eqs 18 and 19 are

a) No azeotrope

$$d_{V,1} < d_{L,1} \text{ and } d_{V,2} < d_{L,2} \tag{20}$$

b) At least one azeotrope of minimum temperature

$$d_{V,1} > d_{L,1} \text{ and } d_{V,2} < d_{L,2} \tag{21}$$

c) At least one azeotrope of maximum temperature

$$d_{V,1} < d_{L,1} \text{ and } d_{V,2} > d_{L,2} \tag{22}$$

d) At least two azeotropes, one of minimum and the other of maximum temperatures

$$d_{V,1} > d_{L,1} \text{ and } d_{V,2} > d_{L,2} \tag{23}$$

Cases b and c are in accordance with the conditions established by Brandani[12] in terms of infinite dilution activity coefficients. The last case presented d is addressed later in this paper, when the presence of more than one azeotrope is considered.

For those cases where, in addition to any of these VLE behaviors, the liquid mixture splits into two liquid phases, these conditions must be combined with a Gibbs energy of mixing curve, $g^{M,L}$, in which a common tangent line at two points must exist. For example, this is the case for the heterogeneous azeotropes (VLLE) that must satisfy the conditions given in eq

21 for the minimum temperature azeotropes (Am) along with a $g^{M,L}$ curve with one common tangent line (LL splitting).

The derivatives $d_{V,1}$ and $d_{V,2}$ depend on the vapor pressures of the two components (1 and 2) of the binary system as shown in eq 17. Thus, the analysis of azeotropy in VLE depends on these values, which are set when the components of the system are specified. In this paper, the procedure that could be carried out to obtain azeotropy and miscibility maps is presented for some of the most used activity coefficient models once the components, and so their vapor pressures, have been set. Table 1 shows the Antoine equation constants

Table 1. Constants for the Antoine Equation (log p_i^0(mmHg) $= A - B/(T(°C) + C)$) for Drawing of Azeotropy Maps Shown in Figures 3 and S8−S10[21]

components	A	B (°C)	C (°C)
light (1): 2-propanol	8.87829	2010.330	252.636
heavy (2): water	8.07131	1730.630	233.426

used in the present work[21] for the calculations that follow, where arbitrarily the parameters for the light (1) and heavy (2) components are those for 2-propanol and water, respectively. The selection of these specific components is not relevant at all to the discussion presented in this paper.

From eq 17 we obtain

$$\frac{dg^{E,V}}{dz_1} = \ln \frac{p_2^0}{p_1^0} \tag{24}$$

that applied at the boiling points of the light ($T_{b,1}$) and heavy ($T_{b,2}$) components provides the required derivatives for the vapor phase:

$$d_{V,1} = \ln\left(\frac{p_2^0}{p_1^0}\right)_{T_{b,1}} \tag{25}$$

$$d_{V,2} = \ln\left(\frac{p_2^0}{p_1^0}\right)_{T_{b,2}} \tag{26}$$

For the liquid phase, the corresponding derivative functions $d_{L,1}$ and $d_{L,2}$ depend on the activity coefficient model. These functions are presented below for the selected models: Margules, van Laar, Wilson, and NRTL. Then, the equalities $d_{V,1} = d_{L,1}$ and $d_{V,2} = d_{L,2}$ have been applied to obtain the limits of azeotropy specified in eqs 20−23.

2.3. Maps of Miscibility and Azeotropy. The adequate combination of the information presented in the previous sections leads to the construction of maps showing the different regions of azeotropy and liquid phase miscibility as functions of the parameter values for some of the most common activity coefficient models. These maps depend on the vapor pressures of the components. As an example, the binary mixture 2-propanol (1) + water (2) has been arbitrarily selected to illustrate the procedure presented in this paper. Constants for the Antoine equation used to calculate the vapor pressures for these two components are given in Table 1.[21]

2.3.1. Margules Equation. From the excess contribution given by the Margules equation, eq 27, eqs 28 and 29 are deduced:

$$g^{E,L} = x_1 x_2 (A_{21} x_1 + A_{12} x_2) \tag{27}$$

$$d_{L,1} = -A_{21} \tag{28}$$

$$d_{L,2} = A_{12} \tag{29}$$

Equating eqs 25 and 28:

$$A_{21} = -\ln\left(\frac{p_2^0}{p_1^0}\right)_{T_{b,1}} \tag{30}$$

which represents a straight line with zero slope (horizontal) in the graphical representation of A_{21} vs A_{12} shown in Figure 3. Below this line, no minimum boiling point azeotrope can be present, and above it, the system will present at least one minimum boiling point azeotrope (Am).
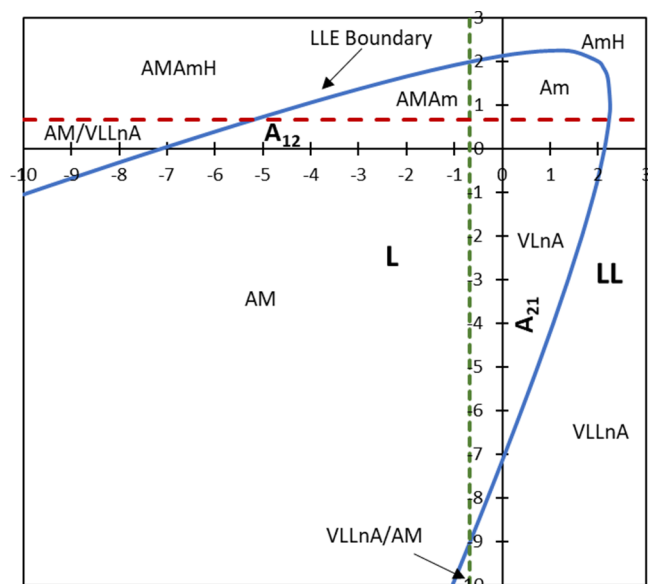

Figure 3. Map showing the different regions for azeotropy and miscibility depending on the parameter values of the Margules equation at atmospheric pressure. Antoine constants in Table 1.

Similarly, equating eqs 26 and 29 is obtained:

$$A_{12} = \ln\left(\frac{p_2^0}{p_1^0}\right)_{T_{b,2}} \tag{31}$$

which represents a straight line with an infinite slope (vertical) in the graphical representation of A_{21} vs A_{12} (Figure 3). To the right of this line, no maximum boiling point azeotrope can exist, while to the left, at least one maximum boiling point azeotrope is present (AM).

This information, combined with the miscibility boundary given in eq 6 that separates the homogeneous (L) and heterogeneous (LL) equilibrium regions, provides the azeotropy and miscibility map represented in Figure 3. This figure shows the variety of equilibrium behaviors that can be obtained with this model as a function of the parameter values. Among them, there are, in addition to the typical nonazeotropic (VLnA) or those presenting one (AM, Am, and AmH) or two (AMAm and AMAmH) azeotropes, other less frequent equilibrium regions as those with nonazeotropic VLL equilibrium, which occurs alone (VLLnA) or combined with a maximum boiling point azeotrope (AM/VLLnA or VLLnA/AM depending on their relative positions with respect to x_1).

A similar procedure has been carried out for the other activity coefficient models, as shown below.

2.3.2. van Laar Equation. From the van Laar equation for the $g^{E,L}$ function (Supporting Information) and applying the required derivatives, the same functions as those using the Margules equation are obtained:

$$d_{L,1} = -A_{21} \tag{32}$$

$$d_{L,2} = A_{12} \tag{33}$$

Thus, equating eqs 25 and 32, on the one hand, and eqs 26 and 33, on the other, two straight lines are obtained, one horizontal and the other vertical, in the graphical representation of A_{21} vs A_{12}. These two lines separate the same azeotropic behaviors as in the Margules equation, but the boundary curves between the L and LL regions are different for each model. In this case, the boundary function for miscibility represented by eq 8 is combined with the azeotropic behavior to provide the map presented in Figure S8 for the van Laar equation. As was already mentioned, in the van Laar equation, both parameters (A_{12} and A_{21}) must have the same sign, and so there are no solutions for the second and fourth quadrants. Moreover, the impossibility of finding solutions to the van Laar equation in the second quadrant (negative A_{12} and positive A_{21} values) prevents the possibility of coexistence of two azeotropes, one of maximum and the other of minimum temperatures (AMAm), for this model. A small region with nonazeotropic VLL equilibrium (VLLnA) is also present in the map for certain values of the parameters.

2.3.3. Wilson Equation. By derivation of the excess contribution given by the Wilson equation (Supporting Information) the following equations are obtained

$$d_{L,1} = -1 + A_{12} + \ln A_{21} \tag{34}$$

$$d_{L,2} = 1 - A_{21} - \ln A_{12} \tag{35}$$

Equating eqs 25 and 34 and rearranging, the following equation is obtained:

$$A_{21} = \exp\left(\ln\left(\frac{p_2^0}{p_1^0}\right)_{T_{b,1}} + 1 - A_{12}\right) \tag{36}$$

Below this curve, represented in Figure S9 (dashed red line), the system forms a minimum boiling point azeotrope (Am), and above it, there are two possibilities: no azeotrope (VLnA) or a maximum boiling point azeotrope (AM). To distinguish between these two situations, it is necessary to operate similarly with eqs 26 and 35, obtaining the following curve (dashed green line)

$$A_{21} = -\ln\left(\frac{p_2^0}{p_1^0}\right)_{T_{b,2}} + 1 - \ln A_{12} \tag{37}$$

which separates the region where both situations, no azeotrope (VLnA) or a minimum boiling point azeotrope (Am), are possible (below) from the one where a maximum boiling point azeotrope (AM) is present (above). The result is the map shown in Figure S9.

Obviously, in this case, it is not possible to represent heterogeneous azeotropes because, as was already mentioned, the Wilson equation does not present the convex/concave transitions required for liquid mixtures splitting (LLE).

Moreover, both A_{12} and A_{21} parameters must be necessarily positive in this model because they are defined as the product between a ratio of volumes and an exponential term, both positives.

2.3.4. NRTL Model. From the Gibbs energy of excess formulated by this model for a binary mixture (Supporting Information), the following derivatives are obtained

$$d_{L,1} = -\tau_{21}G_{21} - \tau_{12} \tag{38}$$

$$d_{L,2} = \tau_{21} + \tau_{12}G_{12} \tag{39}$$

Combining these equations with those for the vapor phase, the boundaries for different azeotropy behaviors are obtained. Thus, by equating eqs 25 and 38, it is obtained:

$$\tau_{12} = -\left(\ln\frac{p_2^0}{p_1^0}\right)_{T_{b,1}} - \tau_{21}G_{21} \tag{40}$$

To the right of this curve (dashed red line in Figure S10), the system presents at least one azeotrope of minimum boiling temperature (Am) and the combination with a maximum boiling point azeotrope (AM) is also possible, providing AMAm behavior. Conversely, to the left of the curve, one of these two possibilities, the absence of azeotropes (VLnA) or a maximum boiling azeotrope (AM), can occur.

Applying the same procedure to eqs 26 and 39, the following is obtained:

$$\tau_{21} = \left(\ln\frac{p_2^0}{p_1^0}\right)_{T_{b,2}} - \tau_{12}G_{12} \tag{41}$$

Above this curve (dashed green line in Figure S10), the system presents either no azeotrope (VLnA) or a minimum boiling point azeotrope (Am). Below, at least one maximum boiling azeotrope (AM) is present, with the possibility of coexistence with a minimum boiling azeotrope (Am) or with nonazeotropic VLL resulting in AMAm and AM/VLLnA types of azeotropy, respectively. All this information has been represented in Figure S10 along with the polynomial function given by eq 9 for the liquid miscibility, providing the different regions for azeotropy and miscibility as a function of the NRTL parameters. Depending on the region for the liquid miscibility behavior, the equilibrium can be VLnA or VLLnA and the azeotropes can be homogeneous or heterogeneous (the last ones identified with H) appearing in new regions in the map, derived from those previously discussed.

2.3.5. Influence of Vapor Pressures on the Azeotropic Behavior. The NRTL model has been arbitrarily selected to illustrate the dependence of the azeotropic behavior on the vapor pressures of the components and the different situations that may occur depending on how similar or dissimilar are their boiling points. In Figure S11, the evolution of the different azeotropic regions with the variation of the vapor pressure of the light component is represented, while the vapor pressure for the heavy component is held constant. Table 2 presents the constants for the Antoine equation used in the calculations for drawing these maps, which were selected arbitrarily to provide the boiling points indicated in the table. The dashed curves that separate the different regions of azeotropic behavior approach each other as the boiling temperatures $T_{b,l}$ and $T_{b,h}$ are closer. This fact causes not only changes in the size of the different regions but also the

Table 2. Constants for the Antoine Equation (log $p_i^0(\text{mmHg}) = A - B/(T(°C) + C)$) Used for Drawing the Maps (NRTL Model) Are Shown in Figure S11

components	A	B (°C)	C (°C)	T_b (°C)
light (1) in Figure S11a	9.0347	1600	230	30
light (1) in Figure S11b	8.5951	1600	230	50
light (1) in Figure S11c	8.2141	1600	230	70
light (1) in Figure S11d	7.8808	1600	230	90
heavy (2)	7.7293	1600	230	100

appearance and disappearance of some of these regions due to the evolution of the intersections between both the miscibility and azeotropy boundaries. This example is intended to illustrate the marked influence of the vapor pressures (of the specific components of the system) on the maps representing the different types of azeotropy and miscibility, which are obtained for some activity coefficient models as a function of their parameters. Related to this, for the Wilson model, it has been found empirically, analyzing different cases, that the combination of two azeotropes is only possible when the difference between the boiling temperatures of the pure components is very small (similar vapor pressures). Moreover, this situation seems to occur exclusively for certain combinations of model parameters where, in addition, the A_{12} parameter is smaller than A_{21}, where 1 is the light component.

2.3.6. Local Maximum or Minimum Boiling Point Azeotropes. The analysis presented, limited to the comparison of the $g^{E,V}$ and $g^{E,L}$ slopes in the extremes of the composition domain ($z_1 = 0$ and $z_1 = 1$) or infinite dilution conditions, explains not only the presence of a unique azeotrope, but also the simultaneous presence of two azeotropes (for a binary system at constant P) when the conditions presented in eq 23 are fulfilled. However, it is important to highlight that these conditions are valid exclusively to detect *global* (maximum or minimum) boiling temperature azeotropes. The *global* or *local* character as maximum or minimum boiling point of azeotropes refers to the comparison between the boiling temperatures of the azeotropes and the pure components. When the system presents only one azeotrope, it is always of *global* maximum or minimum boiling temperature. However, when the system presents more than one azeotrope, it can be *global* or *local* at minimum or maximum boiling temperature. Because *local* (or intermediate) azeotropes are only possible when two or more azeotropes are present, it is in these cases where additional conditions should be established to localize those regions where this type of azeotropes exists. All this with the aim of obtaining more precise maps of azeotropy and miscibility in which these cases are also considered.

Figure 4 schematically shows a possible situation of this type. In this figure, the $g^{M,L}$ and $g^{M,V}$ curves do not satisfy the conditions given by eq 23 (Figure 4a). Even so, the $g^{M,V}$ curves obtained at two intermediate temperatures between $T_{b,l}$ and $T_{b,h}$ are tangent to the $g^{M,L}$ curve, providing one *local* minimum boiling point azeotrope (Figure 4b) and one *local* maximum boiling point azeotrope (Figure 4c), at low and high z_1 mole fraction, respectively. These temperatures have been identified as T_{am} and T_{aM}, where "a" is used for a *local* azeotrope and "amaM" is used to identify the presence of both *local* minimum (am) and maximum (aM) boiling point azeotropes in the system at low and high z_1, respectively. Figure 4d shows the
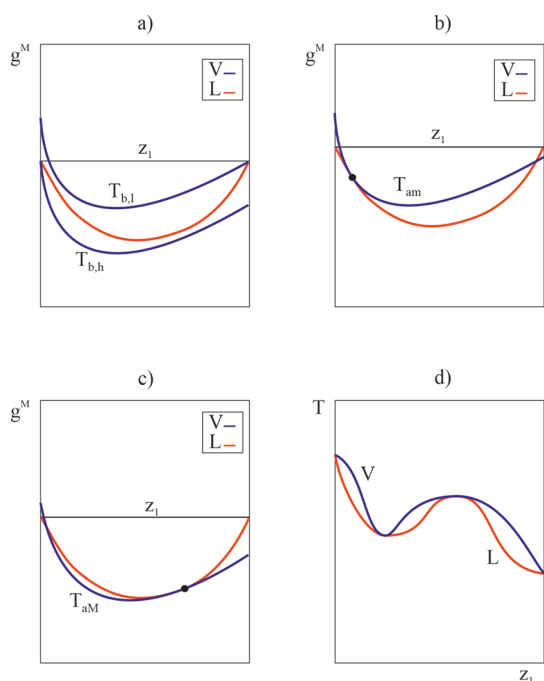
Figure 4. Gibbs energy of mixing curves $g^{M,L}$ and $g^{M,V}$ for a binary system with two homogeneous azeotropes of local minimum and maximum boiling temperatures (amaM) at constant P: (a) $g^{M,V}$ at $T_{b,l}$ and $T_{b,h}$, (b) $g^{M,V}$ at T_{am}, (c) $g^{M,V}$ at T_{aM}, and (d) T/z_1 diagram.

temperature (T) versus composition (z_1) diagram for this type of VLE behavior.

So, if two or more azeotropes could be present in a binary system, the analysis of azeotropy becomes more complicated because the $g^{E,L}$ and $g^{E,V}$ functions, and their derivatives with respect to mole fraction, must be evaluated not only at the extremes ($z_1 = 0$ and $z_1 = 1$) and at the boiling points of the pure components ($T_{b,l}$ and $T_{b,h}$), but also in all of the composition space at any temperature.

In Figure 5, all of the situations that may occur when two azeotropes are present in a binary system at constant P have been represented. There are eight possible combinations of two azeotropes, considering their relative positions (mole fraction) and their local or global character, plus an additional one that is explained later, leading to a total of nine cases (a–i in the figure), of which only six are possible. Figure 5 shows the Gibbs energy of mixing curves for the vapor and liquid phases (1), the excess Gibbs free energy functions (2) and their derivatives (3) also for the vapor and liquid phases, and the T/z_1 diagram (4) illustrating all possible cases. The nomenclature used to name the different types of azeotropes in this figure is the same used previously in this paper: "A" for global and "a" for local maximum (M) or minimum (m) boiling temperature azeotropes. For instance, AmaM would correspond to a system with one global minimum boiling point azeotrope at low z_1 mole fraction and one local maximum boiling point azeotrope at higher z_1 mole fraction.

At this point, two considerations are made that significantly simplify the analysis without modifying the conclusions derived from it. The first one is that, although models such as Wilson and NRTL consider the variation of $g^{M,L}$ with temperature, such variation is generally small, and so the $g^{M,L}$ curve is considered constant with temperature for this analysis. The second question is whether the ratios of the vapor pressures of
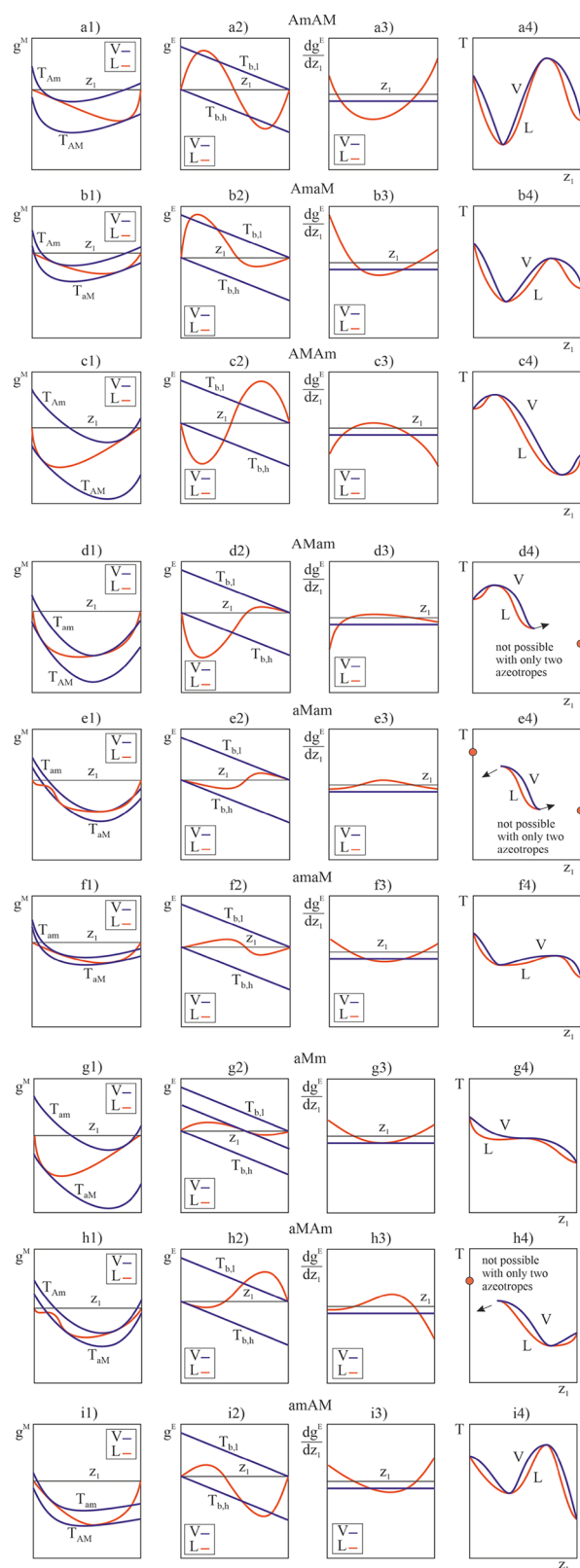

Figure 5. Possible combinations (cases a–i) of two azeotropes in a binary system at constant P, considering their relative positions (mole fraction) and their local or global character as minimum or maximum boiling point azeotropes (compared with the boiling temperatures of the pure components): (1) $g^{M,L}$ and $g^{M,V}$ curves at T of azeotropes, (2) $g^{E,L}$ and $g^{E,V}$ curves at $T_{b,l}$ and $T_{b,h}$, (3) first derivatives of the $g^{E,L}$ and $g^{E,V}$ curves, and (4) T/z_1 diagram.

the two pure components at their boiling point temperatures ($T_{b,l}$ and $T_{b,h}$) that appear in eqs 25 and 26 are very similar, and so, any of them could be considered for the analysis that is carried out. This is the reason why, in column (3) of Figure 5 for all cases a−i, the first derivative of the $g^{E,V}$ curve is a single straight line, without distinguishing between that at $T_{b,l}$ and at $T_{b,h}$ temperatures, which are very close to each other.

It is evident that the systems AMam (case d), aMam (case e), and aMAm (case h) cannot exist if there are only two azeotropes. For instance, the hypothetical aMAm system (Figure 5h) would require a local maximum boiling point near the heavy component of higher boiling temperature. This leads to an absurdity: to the left of the local maximum boiling point, the temperature should decrease, but, otherwise, the temperature should increase to reach the boiling point of the pure heavy component. Similar situations occur in the other two cases in which neither are possible. Besides, Figure 5g shows the particular case, as previously mentioned, where the two intermediate azeotropes merge into a single one. The case presented in Figure 5f is the same as that represented in Figure 4d.

Cases 5a and 5c could be identified by the conditions indicated in eq 23, because they correspond with the two possibilities of combination, AmAM and AMAm, respectively, of the global boiling point (maximum and minimum) azeotropes. However, the other possible cases presented in that figure could not be detected with those conditions because they include some local (instead global) maximum or minimum boiling point azeotrope. A more general condition for detecting all cases, including those where local maximum or minimum boiling point azeotropes are present, is deduced from Figure 5. Thus, from this more general analysis of azeotropy, the following can be stated: *for two azeotropes to be present in a binary system at constant P, the derivatives of the excess Gibbs free energies for the liquid and vapor phases, $g^{E,L}$ and $g^{E,V}$, must have two intersection points between them.* This can be observed in Figure 5a3–i3, except for those not possible cases (d, e, and h) and for case g, where the two intersection points merge into a single one. As the derivative of $g^{E,V}$ is constant (horizontal line), this condition implies that the derivative of $g^{E,L}$ must have a maximum or a minimum. In the first case, the maximum (global or local) boiling point azeotrope appears at the low z_1 mole fraction (case c in Figure 5), and in the second one, it appears at the high z_1 mole fraction (cases a, b, f, and i in Figure 5). However, fulfilling this condition for the presence of two azeotropes is not necessary for the first derivative of $g^{E,L}$ to be zero at two compositions within 0 and 1. This is related to the note published by Jaubert and Privat,[15] where they demonstrated that the presence of a positive (minimum boiling point) or negative (maximum boiling point) azeotrope does not require that g^E for the liquid phase be positive or negative, but concave or convex, respectively. Thus, case b represented in Figure 5, in which both AmaM azeotropes are present, is also possible with a positive $g^{E,L}$ function at any composition (Figure 6 case b2) instead of the one represented in Figure 5 case b2, where negative $g^{E,L}$ values exist in some region where the maximum (local) boiling point azeotrope (aM) is located. The concave part of the $g^{E,L}$ curve allows the minimum (or positive) azeotrope to exist and the convex, *but also positive*, part of the $g^{E,L}$ curve enables the maximum (or negative) azeotrope. Because in this last case, the $g^{E,L}$ curve only presents a maximum, its derivative is only zero at one composition, as it is shown in Figure 6 case b3, unlike Figure 5 case b3, where
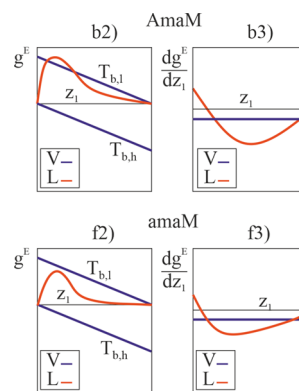

Figure 6. Extension of Figure 5 to show different $g^{E,L}$ curves that provide the same type of azeotropy as those presented in cases b and f: (2) $g^{E,L}$ and $g^{E,V}$ curves at $T_{b,l}$ and $T_{b,h}$ and (3) first derivatives of the $g^{E,L}$ and $g^{E,V}$ curves.

two zeros are present in the derivative due to the presence of both maximum and minimum extremes of the $g^{E,L}$ function (Figure 5 case b2). Jaubert and Privat[15] presented the pentafluoroethane + ammonia system at 49.9 °C as an example of this type of behavior. A similar discussion could be applied to cases f, g, and i, from those possible cases represented in Figure 5. For example, in case f also represented in Figure 6, the presence of amaM azeotropes is also obtained with a positive $g^{E,L}$ function with one concave to convex transition, and so only one zero in its derivative exists. This fact confirms that is the number of intersection points between the derivatives of the g^E functions for the liquid and vapor phases, $g^{E,L}$ and $g^{E,V}$, and not the number of zeros in the derivative of the g^E function for the liquid phase that indicates the number of azeotropes in a binary system. Besides, the composition of these intersection points (i.e., the mole fraction where the derivatives of $g^{E,L}$ and $g^{E,V}$ are equal) is the composition of the azeotropes. In other words, the presence of two azeotropes in a binary system requires a maximum or minimum in the derivative of $g^{E,L}$, and, consequently, one zero in its second derivative. At this point, the mathematical conditions that the system must necessarily fulfill to present an azeotropic behavior of any type can be established as an alternative to those presented by Wisniak et al.[14] Considering these requirements, it is possible to draw some general conclusions, such as that the van Laar model cannot predict two azeotropes because the second derivative of $g^{E,L}$ formulated using this model cannot be zero at any point in the composition interval.

Besides, from Figure 5, it is observed that a local boiling point azeotrope (am or aM) appears when the point where the slopes of the $g^{E,L}$ and $g^{E,V}$ functions are equal is comprised between the straight lines corresponding to the $g^{E,V}$ at the boiling points ($T_{b,l}$ and $T_{b,h}$) of both pure components, as can be seen in cases b (aM at the high z_1 mole fraction), f (am and aM at low and high z_1 mole fractions, respectively), g (aMm at the same mole fraction), and i (am at the low z_1 mole fraction). If those points where the slopes of the $g^{E,L}$ and $g^{E,V}$ functions are equal appear above the $g^{E,V}$ straight line at $T_{b,l}$ or below the $g^{E,V}$ straight line at $T_{b,h}$, the azeotropes are of global minimum (Am) or maximum (AM) boiling temperatures, respectively, as shown in case a (Am and AM at the low and high z_1 mole fraction, respectively), case b (Am at the low z_1 mole fraction), case c (AM and Am at low and high z_1 mole

fractions, respectively), and case i (AM at the high z_1 mole fraction) in Figure 5.

Moreover, it must be considered that the presence of two azeotropes may correspond with the combination of one *heterogeneous* (VLL) and one homogeneous (VL) azeotrope, even though in Figure 5, homogeneous azeotropes have been represented in most cases for simplification. Only in the impossible cases e and h, the $g^{M,L}$ function splits into two liquid phases in equilibrium to enable the required tangencies with the $g^{M,V}$ curve that corresponds to each one of these fictitious situations.

These conditions for azeotropy, which consider the possible presence of local minimum or maximum boiling point azeotropes, have been applied to the Margules equation as an example to illustrate the procedure to obtain a more detailed map of azeotropy and miscibility (Figure 7) than the one previously obtained for this same model (Figure 3).
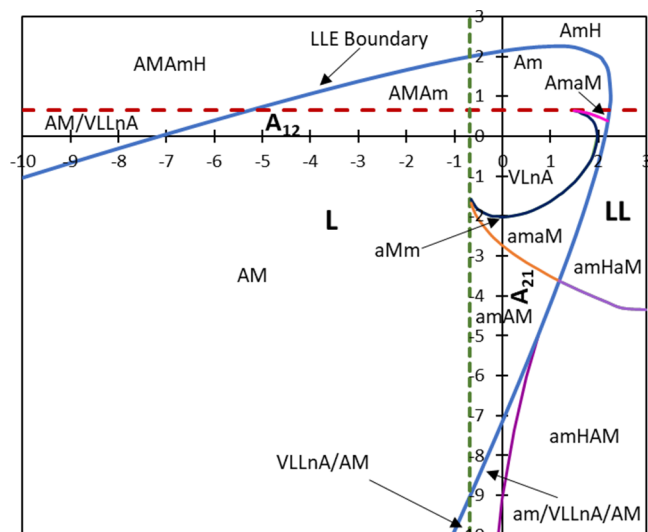

Figure 7. Map showing the different regions for azeotropy and miscibility depending on the parameter values of the Margules equation at atmospheric pressure. Antoine constants are given in Table 1.

It should be noted that in the regions where there were supposedly no azeotropes (VLnA and VLLnA) in Figure 3, now different combinations of azeotropes of local and global character (AmaM, aMm, amaM, amAM, amHaM, amHAM, am/VLLnA/AM) appear (Figure 7). It is due to the limits of azeotropy that have been now obtained evaluating the $g^{E,L}$ and $g^{E,V}$ functions, and their derivatives with respect to mole fraction, in all the composition ranges at each temperature, and not exclusively at the extremes ($z_1 = 0$ and $z_1 = 1$) and at the boiling points of the pure components ($T_{b,l}$ and $T_{b,h}$). For that reason, some limits defining new regions of azeotropy appear in Figure 7, which were not described by eqs 30 and 31 and neither represented in Figure 3.

A more detailed analysis is presented related to two complex regions of the map shown in Figure 7. With that aim, in Figure 8, the T/z_1 diagram for these two regions is shown: the am/VLLnA/AM region (Figure 8a) and the amHAM region (Figure 8b). In the am/VLLnA/AM region, the local minimum point (am) at low z_1 mole fraction is to the left of the VLLnA region (VLLE with no heterogeneous azeotrope), and in the amHAM region, the local minimum boiling point azeotrope is

Figure 8. T/z_1 diagrams for some regions shown in Figure 7 for the Margules equation: (a) am/VLLnA/AM region and (b) amHAM region.

in the VLLE region (heterogeneous azeotrope, amH). Consequently, in the boundary between these two regions, the location of the minimum boiling point azeotrope is exactly at one extreme (low z_1 mole fraction) of the LL tie-line. From the point of view of the Gibbs free energy of mixing, in the am/VLLnA/AM region, the am at low z_1 mole fraction occurs when the tangent point between the $g^{M,L}$ y $g^{M,V}$ curves is to the left of the VLLnA (to the left of the two points on the $g^{M,L}$ curve and one point to the $g^{M,V}$ curve with a common tangent line), while in the amHAM region, the point on the $g^{M,V}$ curve with a common tangent to the LL tie-line is located between them (as Figure S5c shows). So, in the boundary between these two regions, the common tangent point between the $g^{M,L}$ y $g^{M,V}$ curves occurs exactly in one extreme of the LL tie-line. To solve the location of this boundary, the objective function schematically represented by eq 42 could be used:
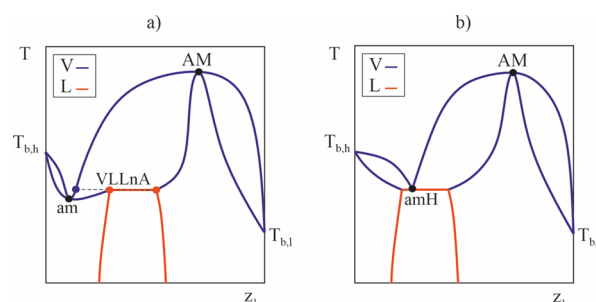
$$\text{F.O} := (\text{F.O.(am)} + \text{F.O.(amH)} + (x_1^{am} - x_1^{1})^2) < \varepsilon \tag{42}$$

where F.O.(am) and F.O.(amH) are the objective functions of the local homogeneous minimum boiling point azeotrope and the local heterogeneous azeotrope, respectively, x_1^{am} is the component 1 mole fraction corresponding to the local minimum boiling point azeotrope (am) and x_1^{I} is the component 1 mole fraction of the liquid phase with low x_1 (phase I) in the heterogeneous azeotrope (amH), and ε is a low tolerance value guaranteeing the fulfillment of the specified conditions. The last of these conditions specified in eq 42 is that the composition of the homogeneous azeotrope (x_1^{am}) must be the same as the composition of one of the liquid phases of the heterogeneous azeotrope (x_1^{I}). In the minimization of this objective function, T and x_1^{I} are the variables to optimize.

Finally, it should be noted that the detailed analysis carried out for the Margules equation, as an example in order to detect the regions that include local maximum or minimum boiling point azeotropes, could be done for any other activity coefficient model in a similar way.

3. CONCLUSIONS

The analysis of the mixing and excess Gibbs free energy functions, and their derivatives with respect to the mole fraction, for both liquid and vapor phases, has led to the development of a procedure for calculating and drawing azeotropy and miscibility maps for binary systems, as a function of the parameter values of some of the most used activity coefficient models (Margules, van Laar, Wilson, and NRTL). The equality to zero of the second and third

derivatives of the $g^{M,L}$ function with respect to the mole fraction, at the same composition, has been the two equations employed to obtain the boundary function between the homogeneous (L) and the heterogeneous (LL) regions as a function of the parameter values of the different activity coefficient models. Besides, the comparative analysis of the slopes of the liquid and vapor excess Gibbs free energies, $g^{E,L}$ and $g^{E,V}$, respectively, evaluated at the extremes of the composition domain ($z_1 = 0$ and $z_1 = 1$) and at the boiling temperatures of the pure components, has allowed us to obtain the required conditions for some of the most common VLE behaviors. However, for systems with two azeotropes that include some local (not global) maximum or minimum boiling point azeotrope (also called intermediate azeotropes), a more general condition must be used: for two azeotropes to be present in a binary system at constant P, the $g^{E,L}$ and $g^{E,V}$ functions must have two intersection points between them, whose compositions are, in addition, those of the azeotropes. These conditions can be easily extended to the presence of three or more azeotropes and systems with three or more components. This study is markedly influenced by the vapor pressures of the pure components. Very different situations may occur depending on how similar or dissimilar their boiling points are and their variation with temperature. So, obtaining a simple expression for relating all variables involved in predicting the existence of different types of azeotropes would be a tough or impossible task. Alternatively, the conditions that the mixing and excess Gibbs free energy functions must fulfill for the different cases are presented in this paper. As an example, a detailed map of azeotropy and miscibility has been obtained as a function of the Margules parameter values for a binary system (2-propanol + water) at atmospheric pressure.

ASSOCIATED CONTENT

ⓢ Supporting Information

The Supporting Information is available free of charge at https://pubs.acs.org/doi/10.1021/acs.iecr.3c03991.

Gibbs energy of mixing and their derivatives for van Laar, Wilson, and NRTL models, parameter values for the boundary between the L and LL regions for the Margules, van Laar, and NRTL equations, and additional representations including maps and conditions for azeotropy and miscibility for different activity coefficient models (PDF)

AUTHOR INFORMATION

Corresponding Author

María del Mar Olaya − *Institute of Chemical Process Engineering, University of Alicante, 03080 Alicante, Spain; Department of Chemical Engineering, University of Alicante, 03080 Alicante, Spain;* ⓞ orcid.org/0000-0001-8068-9562; Email: maria.olaya@ua.es

Authors

Antonio Marcilla − *Institute of Chemical Process Engineering, University of Alicante, 03080 Alicante, Spain; Department of Chemical Engineering, University of Alicante, 03080 Alicante, Spain*

Paloma Carbonell-Hermida − *Institute of Chemical Process Engineering, University of Alicante, 03080 Alicante, Spain;* ⓞ orcid.org/0000-0001-9046-9678

Complete contact information is available at:
https://pubs.acs.org/10.1021/acs.iecr.3c03991

Notes

The authors declare no competing financial interest.

■ NOMENCLATURE

A_{ij}	Binary interaction parameters
A, B, C	Antoine constants
A	Global maximum or minimum boiling point azeotrope
a	Local maximum or minimum boiling point azeotrope
d	Derivative
G^E, g^E	Excess Gibbs free energy (J·mol^{-1}, dimensionless)
$g^{E,L}$	Excess Gibbs free energy of the liquid phase (dimensionless)
$g^{E,V}$	Pseudoexcess contribution to the $g^{M,V}$ function (dimensionless)
g^{ideal}	Ideal Gibbs free energy (dimensionless)
G^M, g^M	Gibbs free energy of mixing (J·mol^{-1}, dimensionless)
H	Heterogeneous (minimum boiling point azeotrope)
LLE	Liquid−liquid equilibrium
M	Maximum boiling point azeotrope
m	Minimum boiling point azeotrope
nA	Nonazeotropic
P	Pressure (Pa or mmHg)
p_i^0	Vapor pressure of component i (Pa or mmHg)
R	Gas constant (J·K^{-1}·mol^{-1})
T	Temperature (K or °C)
T_b	Boiling point (K or °C)
VLE	Vapor−liquid equilibrium
VLLE	Vapor−liquid−liquid equilibrium
x_i	Mole fraction of component i in liquid phase
z_i	Mole fraction of component i in a mixture

■ GREEK SYMBOLS

α_{ij}	Nonrandomness NRTL parameter
γ_i	Activity coefficient of component i
τ_{ij}	NRTL binary interaction parameter (dimensionless)

■ SUPERSCRIPTS

I	One of the two liquid phases at LLE
L	Liquid phase
V	Vapor phase

■ SUBSCRIPTS

0	Equilibrium
1, l	Light component
2, h	Heavy component
i, j	Components
L	Liquid phase
V	Vapor phase

■ REFERENCES

(1) Margules, M. Über Die Zusammensetzung Der Gesättigten Dämpfe von Misschungen. In *Sitzungsber. Akad. Wiss. Wien, math.-naturwiss*; Klasse: Viena, 1895; Vol. 104.

(2) van Laar, J. J. Über Dampfspannungen von Binären Gemischen (The Vapor Pressure of Binary Mixtures). *Z. Phys. Chem.* **1910**, *72*, 723−751.

(3) Wilson, G. M.; Vapor-Liquid Equilibrium, X. I. A New Expression for the Excess Free Energy of Mixing. *J. Am. Chem. Soc.* **1964**, *86* (2), 127−130.

(4) Renon, H.; Prausnitz, J. M. Local Compositions in Thermodynamic Excess Functions for Liquid Mixtures. *AIChE J.* **1968**, *14* (1), 135−144.

(5) *ASPEN-PLUS Chemical Process Optimization Software*; Aspen Technology Inc.: Cambridge, MA.

(6) *CHEMCAD Chemical Process Engineering Software*; Chemstations, Inc.: Houston, TX.

(7) de Klerk, D. L.; Schwarz, C. E. Simplified Approach to Understanding, Evaluating, and Parameterizing the NRTL Model for the Description of Binary VLE: T$\tau\tau$-VLE Approach. *Ind. Eng. Chem. Res.* **2023**, *62*, 10629−10643.

(8) Sapkowski, M.; Hofman, T. Problems and Limitations in the Calculation of Liquid-Liquid Equilibrium. *Fluid Phase Equilib.* **2023**, *571*, No. 113823.

(9) de Klerk, D. L.; Schwarz, C. E. Simplified Approach to the Parameterization of the NRTL Model for Partially Miscible Binary Systems: T$\tau\tau$ LLE Methodology. *Ind. Eng. Chem. Res.* **2023**, *62* (4), 2021−2035.

(10) Brito Alves, R. M.; Quina, F. H.; Oller Nascimento, C. A. New Approach for the Prediction of Azeotropy in Binary Systems. *Comput. Chem. Eng.* **2003**, *27* (12), 1755−1759.

(11) Li, A. H.; Paluch, A. S.; Liu, Z. Y. Prediction of Azeotrope Formation in Binary Mixtures with Pure Component Properties and Limiting Activity Coefficients. *Fluid Phase Equilib.* **2023**, *565*, No. 113664.

(12) Brandani, V. Use of Infinite-Dilution Activity Coefficients for Predicting Azeotrope Formation at Constant and Partial Miscibility in Binary Liquid Mixtures. *Ind. Eng. Chem. Fundamen* **1974**, *13*, 154−156.

(13) Gmehling, J.; Kleiber, M. Vapor−Liquid Equilibrium and Physical Properties for Distillation. In *Distillation: Fundamentals and Principles*; Academic Press, 2014; pp. 45−95.

(14) Wisniak, J.; Segura, H.; Reich, R. *Polyazeotropy in Binary Systems*, 1996. https://pubs.acs.org/sharingguidelines.

(15) Jaubert, J. N.; Privat, R. Possible Existence of a Negative (Positive) Homogeneous Azeotrope When the Binary Mixture Exhibits Positive (Negative) Deviations from Ideal Solution Behavior (That Is, When GE Is Positive (Negative)). *Ind. Eng. Chem. Res.* **2006**, *45* (24), 8217−8222.

(16) Bonilla-Petriciolet, A.; Iglesias-Silva, G. A.; Hall, K. R. Calculation of Homogeneous Azeotropes in Reactive and Non-Reactive Mixtures Using a Stochastic Optimization Approach. *Fluid Phase Equilib.* **2009**, *281* (1), 22−31.

(17) Skiborowski, M.; Bausa, J.; Marquardt, W. A Unifying Approach for the Calculation of Azeotropes and Pinch Points in Homogeneous and Heterogeneous Mixtures. *Ind. Eng. Chem. Res.* **2016**, *55* (24), 6815−6834.

(18) Reyes-Labarta, J. A.; Olaya, M. M.; Velasco, R.; Serrano, M. D.; Marcilla, A. Correlation of the Liquid-Liquid Equilibrium Data for Specific Ternary Systems with One or Two Partially Miscible Binary Subsystems. *Fluid Phase Equilib.* **2009**, *278* (1−2), 9−14.

(19) Marcilla Gomis, A.; Reyes-Labarta, J. A.; Serrano Cayuelas, M. D.; Olaya López, M. M. GE Models and Algorithms for Condensed Phase Equilibrium Data Regression in Ternary Systems: Limitations and Proposals. *Open Thermodynamics Journal* **2011**, *5* (1), 48−62.

(20) Labarta, J. A.; Olaya, M. M.; Marcilla, A. F. What Does the NRTL Model Look like? Determination of Boundaries for Different Fluid Phase Equilibrium Regions. *AIChE J.* **2022**, *68*, No. e17805.

(21) Gmehling, J.; Onken, U.; Rarey-Nies, J. R. *Vapor-Liquid Equilibrium Data Collection*; Chemistry Data Series, Vol I. Part 1b: Aqueous Systems Supplement 2; DECHEMA: Frankfurt, Germany, 1988.